

Why R-Homocitrate Is Essential to the Reactivity of FeMo-Cofactor of Nitrogenase: Studies on NifV⁻-Extracted FeMo-Cofactor

Karin L. C. Grönberg, Carol A. Gormal, Marcus C. Durrant, Barry E. Smith, and Richard A. Henderson*

Contribution from the John Innes Centre, Nitrogen Fixation Laboratory, Norwich Research Park, Colney, Norwich NR4 7UH, U.K.

Received May 26, 1998

Abstract: The dinitrogen-binding site in the Mo-based nitrogenase is FeMo-cofactor, a metallo-sulfur cluster of composition MoFe₇S₉·R-homocitrate. The NifV⁻ mutant nitrogenase from *Klebsiella pneumoniae* contains an FeMo-cofactor in which homocitrate has been replaced by citrate (i.e., MoFe₇S₉·citrate). Both the wild type and mutant cofactors (in the $S = 3/2$ spin state) can be extracted into *N*-methylformamide. The extracted cofactors bind one molecule of PhS⁻ at the tetrahedral Fe, and the rate of this reaction depends on what else is coordinated to the cluster. No differences were observed between the reactivities of wild-type and NifV⁻ cofactors with PhS⁻ when they were complexed with CN⁻, N₃⁻, or H⁺. However, when imidazole is bound, the kinetics of the reactions of PhS⁻ with the two cofactors are very different. Here we propose that R-homocitrate (but not citrate) can hydrogen bond to the imidazole ligand on Mo, and that this perturbs the electron distribution within the cluster core, and hence its reactivity with PhS⁻. Using the X-ray crystallographic data for the MoFe-protein of nitrogenase and molecular mechanics calculations, we have investigated the implications of these findings on the action of the enzyme. Our model shows that R-homocitrate is uniquely capable of facilitating the binding of dinitrogen by allowing the substrate access to Mo after dissociation of the Mo–carboxylate bond while simultaneously influencing the electron-richness of the cofactor by hydrogen bonding of the pendant –CH₂CH₂CO₂ arm to the imidazole group of Hisα442. The whole process is mediated by hydrogen bonding of amino acid side chains to the carboxylate groups of R-homocitrate.

Introduction

Nitrogenases are the enzymes which convert dinitrogen into ammonia by a sequence of coupled electron- and proton-transfer reactions,¹ and they are also capable of transforming a variety of other species, including CN⁻, N₃⁻, MeNC, C₂H₂, N₂O, and H⁺. The Mo-based enzyme consists of two metalloproteins: (i) the Fe-protein, which mediates electron-transfer from a flavodoxin or ferredoxin to (ii) the MoFe-protein, where dinitrogen is bound and transformed at the FeMo-cofactor. The FeMo-cofactor is an Fe–S-based cluster of composition MoFe₇S₉·R-homocitrate (Figure 1) which has been structurally characterized by X-ray crystallography in *Azotobacter vinelandii*.² The FeMo-cofactor is ligated to the polypeptide at only two positions: through a cysteinate sulfur (Cysα275) to the unique tetrahedral Fe (all other Fe's are three coordinate) and through a histidine residue (Hisα442) to the Mo.

The way in which this cluster binds and activates dinitrogen, or any of the other substrates, is still obscure, but it is clear that the cluster alone cannot do this chemistry: amino acid side chains, close to the cofactor, are intimately involved in this transformation. Thus, studies on mutant nitrogenases have shown that even small changes to the environment of the cluster can affect the nitrogen fixing ability of the enzyme.^{3,4} In this

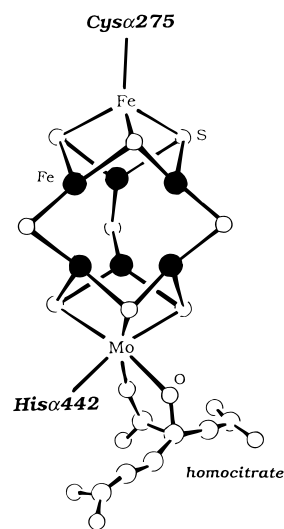


Figure 1. FeMo-cofactor: the substrate binding site of nitrogenase. In this paper, we will concentrate on the mutation of the *nifV* gene (which encodes a homocitrate synthase⁵), which results in biosynthesis of the NifV⁻ nitrogenase, an enzyme with a very low nitrogen fixing ability. In *Klebsiella pneumoniae*, this mutant cofactor has citrate rather than R-homocitrate bound to the Mo (i.e., MoFe₇S₉·citrate).⁶

(1) Burgess, B. K.; Lowe, D. J. *Chem. Rev.* **1996**, *96*, 2983 and references therein.

(2) Howard, J. B.; Rees, D. C. *Chem. Rev.* **1996**, *96*, 2965 and references therein.

(3) Scott, J. D.; Dean, D. R.; Newton, W. E. *J. Biol. Chem.* **1992**, *267*, 20002.

(4) Kim, C.-H.; Newton, W. E.; Dean, D. R. *Biochemistry* **1995**, *34*, 2793.

(5) Hoover, T. R.; Robertson, A. D.; Cerny, R. L.; Hayes, R. N.; Imperial, J.; Shah, V. K.; Ludden, P. W. *Nature* **1987**, *329*, 855. Zheng, L.; White, R. H.; Dean, D. R. *J. Bacteriol.* **1997**, *179*, 5963.

(6) Liang, J.; Madden, M.; Shah, V. K.; Burris, R. H. *Biochemistry* **1990**, *29*, 8577.

The FeMo-cofactors (in the $S = 3/2$ spin state) from both the wild-type and mutant nitrogenases can be extracted, as extremely oxygen-sensitive clusters, from the MoFe-proteins into *N*-methylformamide (NMF) containing water (ca. 5% molar concentration), phosphate buffer, and sodium dithionite.⁷ During the extraction, the cysteine and histidine ligands dissociate from the cofactor and are, presumably, replaced by NMF. There is good evidence from EXAFS spectroscopy (as reviewed by Howard and Rees²) that the cluster structure of FeMo-cofactor is maintained upon extraction, with the Fe···Fe and Mo···Fe distances remaining the same within experimental error.

We now report the first comparative kinetic studies on the reactivities of extracted wild-type and *NifV*⁻ cofactors and show that the two clusters have different reactivities only when imidazole is bound to the cluster. The results of this work suggest a novel role for the R-homocitrate ligand in “tuning” the reactivity of the cofactor in the enzyme during turnover. We have explored this possibility using molecular mechanics calculations on the crystal structure of the MoFe-protein of nitrogenase.

Experimental Section

All manipulations involving the preparation of samples of extracted cofactor for stopped-flow studies were performed under an atmosphere of dinitrogen in an anaerobic glovebox ($O_2 < 1$ ppm).

Preparation of Materials. The nitrogenase MoFe proteins were purified from wild-type *K. pneumoniae* M5a1 and the *nifV* mutant *K. pneumoniae* strain UNF 837, and the respective FeMo-cofactors were isolated and assayed using minor modifications of the methods described earlier.^{8,9}

[NEt₄]SPh was prepared by the literature method¹⁰ and recrystallized from MeCN/Et₂O.

[NHET₃]BPh₄ was prepared by the literature method.¹¹

Imidazole, [NEt₄]CN, and NaN₃ were purchased from Aldrich and used as received.

NMF was purchased from Aldrich, dried over anhydrous sodium carbonate, and distilled under reduced pressure.

Kinetic Studies. Solutions of FeMo-cofactor for the kinetic studies (1×10^{-4} mol dm⁻³) were prepared in a glovebox using NMF containing sodium dithionite (1×10^{-3} mol dm⁻³ added in aqueous solution containing phosphate buffer). In experiments where CN⁻, N₃⁻, or imidazole is added to FeMo-cofactor, 8 mol equiv of the reagent was added to the FeMo-cofactor solution. The dilute solution was loaded into a 5-mL all-glass syringe inside the glovebox and stoppered using a needle attached to a rubber bung. The sealed syringes were then removed from the glovebox and the solutions loaded into a stopped-flow apparatus without allowing air to come in contact with the solutions. The kinetics of the reaction between extracted FeMo-cofactor and [NEt₄]SPh in NMF were studied on a Hi-Tech SF-51 stopped-flow apparatus, modified to handle air-sensitive materials.¹² The temperature was maintained at 25.0 °C using a Grant LE8 thermostat tank. The stopped-flow spectrophotometer was connected to a Viglen computer via an analog-to-digital converter. The kinetics were studied at $\lambda = 450$ or 475 nm. Under all conditions, the initial absorbance is that of extracted FeMo-cofactor, and the final absorbance is that of the PhS derivative. The values of the observed rate constants (k_{obs}) were determined by curve-fitting of the exponential absorbance–time curve using a computer program.

(7) Burgess, B. K. *Chem. Rev.* **1990**, *90*, 1377 and references therein.

(8) Richards, A. J. M.; Lowe, D. J.; Richards, R. L.; Thomson, A. J.; Smith, B. E. *Biochem. J.* **1994**, *297*, 373 and references therein.

(9) Hawkes, T. R.; McLean, P. A.; Smith, B. E. *Biochem. J.* **1984**, *217*, 317 and references therein.

(10) Palermo, R. E.; Power, P. P.; Holm, R. H. *Inorg. Chem.* **1982**, *21*, 173.

(11) Dilworth, J. R.; Henderson, R. A.; Dahlstrom, P.; Nicholson, T.; Zubieta, J. A. *J. Chem. Soc., Dalton Trans.* **1987**, 529.

(12) Henderson, R. A. *J. Chem. Soc., Dalton Trans.* **1982**, 917.

It has been proposed¹³ that extracted FeMo-cofactor oligomerizes in NMF solution. We see no evidence of this in our kinetic studies. Varying the concentration of FeMo-cofactor ($[FeMo-co] = 0.2\text{--}0.025$ mmol dm⁻³), while keeping the concentration of PhS⁻ constant, does not affect the value of k_{obs} .

Molecular Modeling Studies. Molecular mechanics calculations (using the MM2 force field) were carried out using ChemX software¹⁴ and the published X-ray crystal structure coordinates for nitrogenase.¹⁵ All modeling studies were carried out on the A and B subunits of the $\alpha_2\beta_2$ tetramer, as given in the X-ray coordinate set. Water molecules were not included. The MoFe₇S₉ moiety and the bulk of the protein, including all of the atoms in the protein backbone, were left unmodified. Hydrogen atoms were added as required in calculated positions. Since the noncoordinated carboxylates of the homocitrate moiety were markedly nonplanar in the crystal structure of the MoFe-protein¹⁵ as received, these were reconstructed to idealized geometries.

Results and Discussion

The Approach. Studies on extracted FeMo-cofactors allow us to answer questions about the intrinsic reactivity associated with the free clusters. It has been known for some time that extracted FeMo-cofactor is incapable of fixing dinitrogen,⁷ but several spectroscopic studies have indicated that some of the other substrates of nitrogenase, such as CN⁻, N₃⁻, MeNC, and H⁺, can bind to this cluster.^{8,16–19}

In an extension of our work on synthetic Fe–S-based clusters,²⁰ we have developed a simple method to monitor the binding of molecules or ions to the cofactor, using one of the simplest reactions of extracted FeMo-cofactor: the reaction with PhS⁻ (Figure 2).

We have already reported kinetic studies on the reaction between PhS⁻ and extracted wild-type FeMo-cofactor.²¹ Briefly, the binding of PhS⁻ to the unique tetrahedral Fe on extracted wild-type cofactor^{22,23} can be studied using anaerobic stopped-flow spectrophotometry. The reaction occurs at a rate which shows a first-order dependence on the concentration of extracted cofactor but is independent of the concentration of PhS⁻ ($k^{\text{NMF}} = 50 \pm 7$ s⁻¹). These kinetics are consistent with a mechanism involving rate-limiting dissociation of the Fe–NMF bond, followed by the rapid binding of PhS⁻. Consequently, the rate

(13) Huang, H. Q.; Kofford, M.; Simpson, F. B.; Watt, G. D. *J. Inorg. Biochem.* **1993**, *52*, 59.

(14) ChemX, Chemical Design Ltd., Oxon., England, July 1996.

(15) Peters, J. W.; Stowell, M. H. B.; Soltis, S. M.; Finnegan, M. G.; Johnson, M. K.; Rees, D. C. *Biochemistry* **1997**, *36*, 1181; Brookhaven Protein Data Bank ref 3MIN.

(16) Conradson, S. D.; Burgess, B. K.; Vaughan, S. A.; Roe, A. L.; Hedman, B.; Hodgson, K. O.; Holm, R. H. *J. Biol. Chem.* **1989**, *264*, 15967 and references therein.

(17) Liu, H. I.; Filippini, A.; Gavini, N.; Burgess, B. K.; Hedman, B.; Di Cicco, A.; Natoli, C. R.; Hodgson, K. O. *J. Am. Chem. Soc.* **1994**, *116*, 2418.

(18) Richards, A. J. M. Ph.D. Thesis, University of East Anglia, 1986.

(19) (a) Schultz, F. A.; Feldman, B. J.; Gheller, S. F.; Newton, W. E. *Inorg. Chim. Acta* **1990**, *170*, 115. (b) Newton, W. E.; Gheller, S. F.; Feldman, B. J.; Dunham, W. R.; Schultz, F. A. *J. Biol. Chem.* **1989**, *264*, 1924.

(20) Grönberg, K. L. C.; Henderson, R. A.; Oglieve, K. E. *J. Chem. Soc., Dalton Trans.* **1997**, 1507 and references therein.

(21) Grönberg, K. L. C.; Gormal, C. A.; Smith, B. E.; Henderson, R. A. *J. Chem. Soc., Chem. Commun.* **1997**, 713.

(22) EXAFS studies have shown that the thiolate binds to an Fe atom. This is almost certainly the unique tetrahedral Fe, since this site has a natural affinity for binding a thiolate (cysteinate) in the MoFe-protein. Newton, W. E.; Gheller, S.; Schultz, F. A.; Burgess, B. K.; Conradson, S. D.; McDonald, J. W.; Hedman, B.; Hodgson, K. O. In *Nitrogen Fixation Research Progress*; Evans, H. J., Bottomley, P. J., Newton, W. E., Eds.; Martinus Nijhoff: Dordrecht, The Netherlands, 1985; p 604.

(23) Harvey, I.; Strange, R. W.; Schneider, R.; Gormal, C. A.; Garner, C. D.; Hasnain, S. S.; Richards, R. L.; Smith, B. E. *Inorg. Chim. Acta* **1998**, *275–276*, 150.

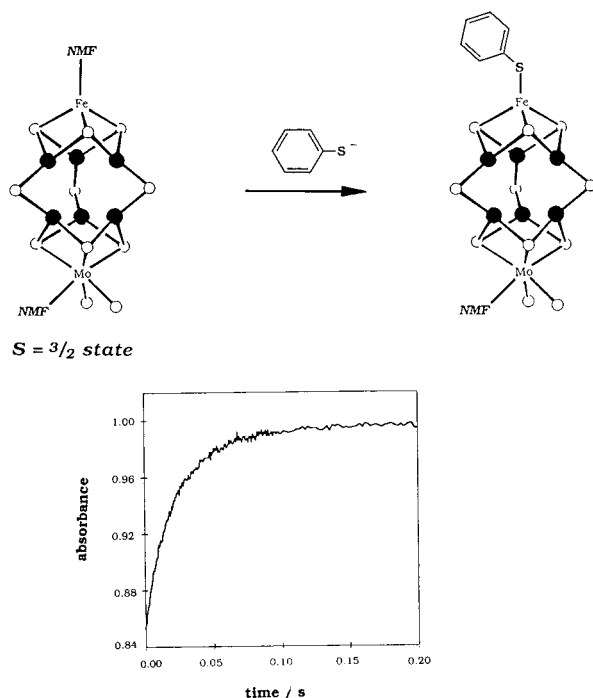


Figure 2. Reaction of PhS⁻ with extracted FeMo-cofactor and a typical stopped-flow absorbance–time curve for this reaction. [FeMo-co] = 0.1 mmol dm⁻³; [PhS⁻] = 20.0 mmol dm⁻³; λ = 450 nm in NMF at 25.0 °C.

of this substitution reaction is, to a large extent, controlled by the strength of the Fe–NMF bond. We can use this reaction to give us information about other interactions occurring elsewhere on the cofactor.

The approach taken is as follows: if a molecule or ion binds to extracted FeMo-cofactor, it will perturb the electron distribution within the cluster, and this will affect the strength of the Fe–NMF bond and, hence, the rate of the reaction with PhS⁻. Thus, the rate of the reaction between PhS⁻ and extracted FeMo-cofactor is sensitive to what else is bound to the cluster. Effectively, the rate of the reaction with PhS⁻ “reports” on the interaction of cofactor with other molecules and ions. We have already shown that the reaction of wild-type cofactor with PhS⁻ is (i) dramatically inhibited by the binding of CN⁻, (ii) slightly inhibited by Bu^tNC, (iii) slightly accelerated by N₃⁻ or imidazole, and (iv) accelerated by the addition of H⁺. This behavior is consistent with CN⁻ binding at, or close to, the tetrahedral Fe, H⁺ binding to a bridging sulfur (or possibly the R-homocitrate ligand), and all other molecules binding at, or close to, Mo.²¹

We have now used this reaction of cofactor with PhS⁻ to compare the effects that coordinated R-homocitrate or citrate have on the reactivity of extracted cofactors.

Reactivity of NifV⁻ Mutant Cofactor. R-Homocitrate is a bidentate ligand to the Mo of wild-type FeMo-cofactor; ligating via an alkoxy and a carboxylato group (Figure 1). The R-homocitrate is made by a homocitrate synthase which is encoded by the *nifV* gene.⁵ Mutation of this *nifV* gene results in a mutant cofactor which (at least for *K. pneumoniae*) has citrate bound to Mo (Figure 3).

Although we have no crystallographic information about the mode of binding of citrate, it is reasonable to assume that it binds via alkoxy and carboxylato groups in a fashion analogous to that of R-homocitrate. Binding in this manner produces a five-membered chelate ring, while any other ligation would involve thermodynamically less stable larger chelate rings. The

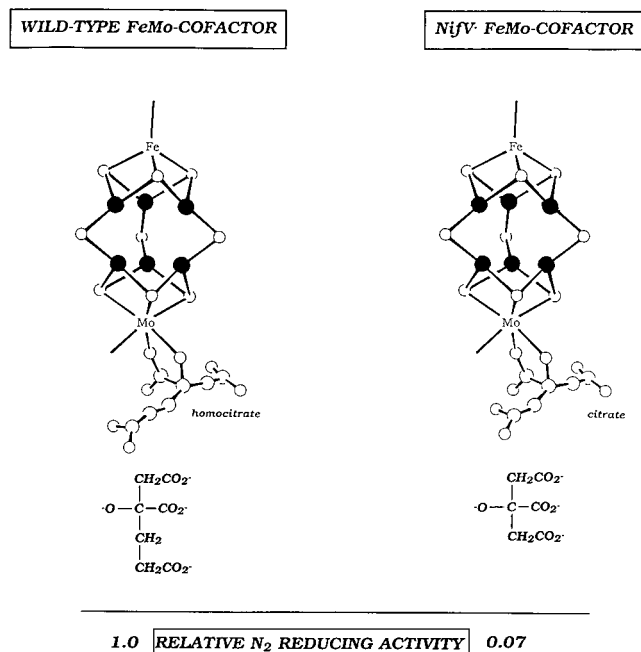


Figure 3. Comparison of the structures and nitrogen fixing ability of the wild-type (LHS) and NifV⁻ (RHS) cofactors.

results we present in this paper (vide infra) show that (except in the presence of imidazole) the reactivities of wild-type and NifV⁻-extracted cofactors with PhS⁻ are indistinguishable. This is entirely consistent with the proposition that R-homocitrate and citrate are bound in analogous ways.

Chemically, the citrate-for-homocitrate replacement appears trivial: the only difference between citrate and homocitrate is that the latter contains an extra CH₂ group. However, as can be seen in Figure 3, this group is not involved in the ligation to the cluster. Rather, it is part of the pendant CH₂CH₂CO₂ arm which hangs free from the cofactor. Nonetheless, this substitution of citrate for homocitrate has a dramatic effect on the nitrogen-fixing ability of the enzyme: the NifV⁻ mutant enzyme is only ca. 7% as good at fixing dinitrogen as the wild-type nitrogenase.⁹ Biochemical studies²⁴ have shown that the identity of the polycarboxylate ligand is crucial in facilitating nitrogen fixation. The protein-bound FeMo-cofactor is competent in dinitrogen fixation only if the polycarboxylate ligand has the following components: (i) 1- and 2-carboxyl groups, (ii) a hydroxyl group, (iii) an R-configuration, and (iv) a carbon chain length of four to six atoms with two carboxyl groups. Until now, there has been no chemical rationale for this specificity.

To investigate whether the difference in the nitrogen fixing ability of wild-type and NifV⁻ nitrogenases is reflected in the intrinsic reactivity of the cluster, the mutant cofactor from the NifV⁻ enzyme has been extracted and the kinetics of its reaction with PhS⁻ studied. Clearly, the rate of this reaction with PhS⁻ does not directly relate to the nitrogen fixing ability of the cofactors. However, this rate is extremely sensitive to electronic effects within the cluster, effects which are likely to be important in the fixation process. The effect that other species, such as CN⁻, N₃⁻, H⁺, or imidazole, have on the extracted cofactors has been compared.

The reactivities of the extracted mutant and wild-type cofactors are very similar. Thus, the reaction of NifV⁻ cofactor with an excess of PhS⁻ occurs at a rate which exhibits a first-order dependence on the concentration of cofactor but is

(24) Imperial, J.; Hoover, T. R.; Madden, M. S.; Ludden, P. W.; Shah, V. K. *Biochemistry* **1989**, *28*, 7796.

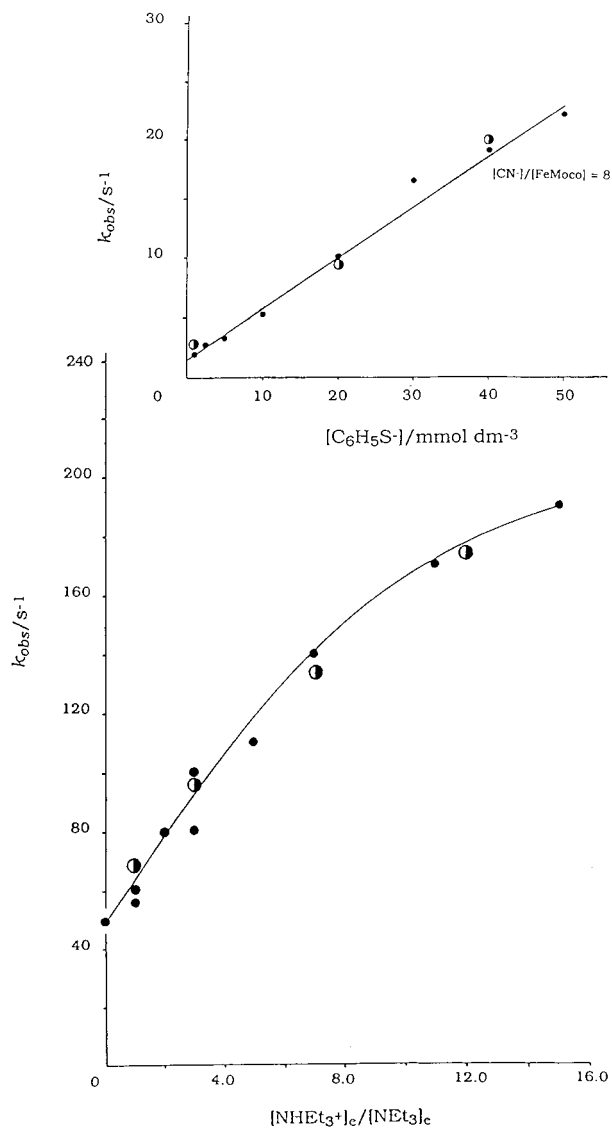


Figure 4. Influence of $[\text{NHEt}_3^+]/[\text{NEt}_3]$ on k_{obs} for the reaction between FeMo-cofactor and PhS^- . Data points correspond to wild-type (●) and NifV⁻ (○) cofactors. Curve drawn is that defined by the data for the wild-type cofactor,²¹ where $K^{\text{H}} = 0.056$ and $k_1^{\text{H}} = 312 \text{ s}^{-1}$: $k_{\text{obs}} = \{k_1^{\text{H}}K^{\text{H}}[\text{NHEt}_3^+]/[\text{NEt}_3]\}/\{1 + K^{\text{H}}[\text{NHEt}_3^+]/[\text{NEt}_3]\}$. This rate law is consistent with a mechanism involving rapid protonation of the cofactor (K^{H}), followed by rate-limiting dissociation of the Fe–NMF bond (k_1^{H}). The site of protonation is most probably either a bridging sulfur or an oxygen on the polycarboxylate ligand. Inset (top): Influence of the concentration of PhS^- on k_{obs} for the reaction between FeMo-cofactor in the presence of 8 mol equiv of CN^- . Data points correspond to wild-type (●) and NifV⁻ (○) cofactors. Line drawn is that defined by the data for the wild-type cofactor,²¹ where $k_1^{\text{CN}} = 1.35 \text{ s}^{-1}$ and $k_2^{\text{CN}} = 4.3 \times 10^2 \text{ dm}^3 \text{ mol}^{-1} \text{ s}^{-1}$: $k_{\text{obs}} = k_1^{\text{CN}} + k_2^{\text{CN}}[\text{PhS}^-]$. This rate law is consistent with the mechanism shown in ref 21, involving cyanide binding to FeMo-cofactor at the tetrahedral Fe and displacement by PhS^- occurring via dissociative (k_1^{CN}) and associative (k_2^{CN}) pathways.

independent of the concentration of PhS^- ($k_{\text{obs}} = 50 \pm 5 \text{ s}^{-1}$), indistinguishable from that of the wild-type cofactor. In addition, when CN^- , N_3^- , or H^+ is bound to NifV⁻ cofactor, the kinetic data for the reactions with PhS^- are indistinguishable from those of the analogous reactions of wild-type cofactor (Figure 4). This is what one would expect. As far as the cofactor cluster core is concerned, citrate looks like, and has an electronic influence similar to, homocitrate. However, there is one molecule which, when bound to the two cofactors, results

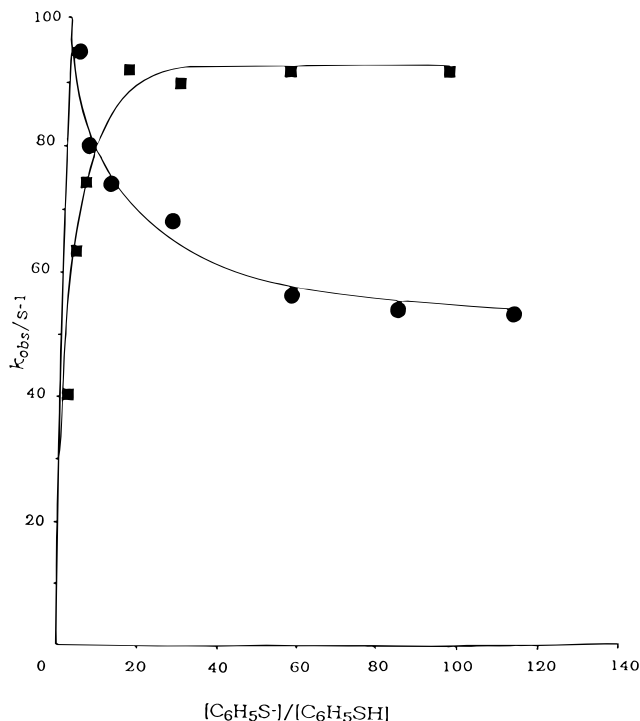


Figure 5. Comparison of the influence of $[\text{PhS}^-]/[\text{PhSH}]$ on k_{obs} for the reactions of PhS^- with NifV⁻ FeMo-cofactor (■) and wild-type FeMo-cofactor (●) in the presence of imidazole. Curves drawn are those defined by eq 1, together with the parameters given in the text.

in very different reactivities of the two clusters. That molecule is imidazole.

The kinetics of the substitution reaction of PhS^- with NifV⁻ cofactor in the presence of imidazole show a first-order dependence on the concentration of the cofactor, but now the rate varies with the concentration of PhS^- . Varying the concentrations of PhS^- and PhSH shows that, strictly speaking, the rate varies with the ratio $[\text{PhS}^-]/[\text{PhSH}]$ as shown in Figure 5.

It is only in the presence of imidazole that the rate of reaction depends on $[\text{PhS}^-]/[\text{PhSH}]$. This is readily understood in terms of the acid–base chemistry of coordinated imidazole. PhS^- has two roles in the reaction with extracted FeMo-cofactor in the presence of imidazole: (i) it is the nucleophile for the substitution reaction at the Fe site, and (ii) PhS^- is a sufficiently strong base in NMF that, at high concentrations, it is capable of deprotonating coordinated imidazole to form an imidazolate–FeMo-cofactor species. Thus, the nonlinear dependence on $[\text{PhS}^-]/[\text{PhSH}]$ (Figure 5) is caused by deprotonation of the imidazole ligand: at low $[\text{PhS}^-]/[\text{PhSH}]$, the cofactor has imidazole coordinated, while at high $[\text{PhS}^-]/[\text{PhSH}]$, the cofactor has imidazolate bound (Figure 6). Whether the proton is bound to the imidazole or not affects the electron distribution within the cluster and, hence, the rate of the substitution reaction with PhS^- . It is solely this protolytic equilibrium which gives rise to the dependence of the rate on $[\text{PhS}^-]/[\text{PhSH}]$. Although PhS^- is also the nucleophile for the substitution reaction occurring at the tetrahedral Fe, this process is still rate-limited by dissociation of the Fe–NMF bond, and thus the elementary act of substitution occurs at a rate independent of the concentration of PhS^- .

Confirmation that the effects being observed are associated with acid–base behavior of coordinated imidazole comes from studies on wild-type cofactor in the presence of *N*-methylimidazole. The absence of an ionizable proton in this derivative

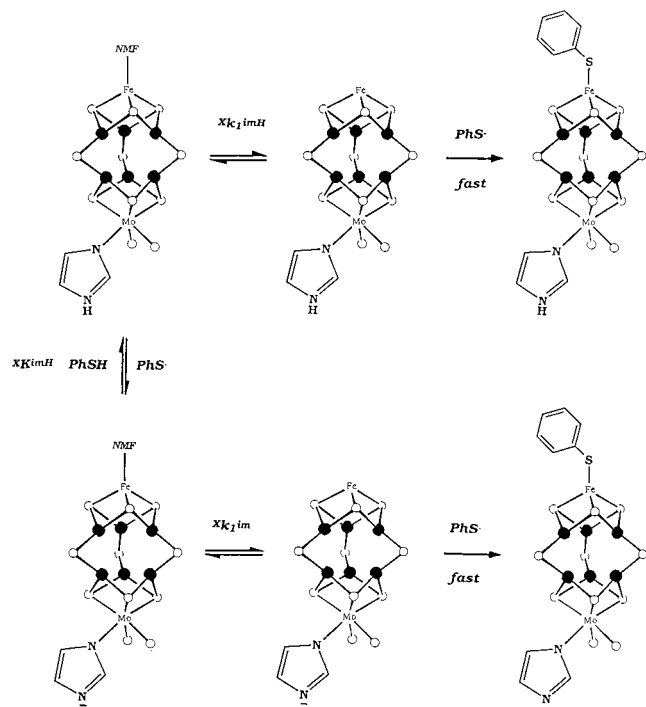


Figure 6. Mechanism for the reaction of PhS⁻ with extracted FeMo-cofactor in the presence of imidazole.

results in the reaction with PhS⁻ occurring at a rate which shows a first-order dependence on the concentration of cofactor ($k_{\text{obs}} = 60 \pm 5 \text{ s}^{-1}$) but, most crucially, is independent of [PhS⁻]/[PhSH].

The mechanism for the reaction between extracted FeMo-cofactor and PhS⁻, in the presence of imidazole, is shown in Figure 6, and the rate law derived from this mechanism is shown in eq 1.

$$\frac{-d[\text{FeMoco}]}{dt} = \frac{\{Xk_1^{\text{imH}} + Xk_1^{\text{im}}(XK^{\text{imH}})[\text{PhS}^-]/[\text{PhSH}]\}[\text{FeMo-co}]}{1 + XK^{\text{imH}}[\text{PhS}^-]/[\text{PhSH}]} \quad (1)$$

For the NifV⁻ extracted FeMo-cofactor ($X = \text{V}$), ${}^{\text{V}}k_1^{\text{imH}} = 30 \pm 5 \text{ s}^{-1}$; ${}^{\text{V}}k_1^{\text{im}} = 95 \pm 5 \text{ s}^{-1}$, and ${}^{\text{V}}K^{\text{imH}} = 0.35 \pm 0.02$. From a chemical point of view, the reactivity pattern observed in this study seems intuitively correct. The imidazolite-FeMo-cofactor is more labile to substitution than the imidazole form because the imidazolite ligand is negatively charged and would be more electron-releasing than imidazole. Releasing electron density into the cluster facilitates the rate-limiting dissociation of the Fe–NMF bond.

Comparison of NifV⁻ and Wild-Type Cofactors. Comparing the reactivity of the extracted mutant cofactor with that of wild-type cofactor, in the presence of imidazole, we see a marked difference between the two clusters (Figure 5). As with the mutant cofactor, the reaction of wild-type cofactor shows a first-order dependence on the concentration of cofactor and a nonlinear dependence on [PhS⁻]/[PhSH].²¹ However, there are two clear differences. (i) With wild-type cofactor, the rate *decreases* as [PhS⁻]/[PhSH] increases. This behavior is consistent with the mechanism shown in Figure 6 and the rate law of eq 1. The derived values of the elementary rate constants and equilibrium constants with wild-type cofactor ($X = \text{WT}$) are ${}^{\text{WT}}k_1^{\text{imH}} = 95 \pm 5 \text{ s}^{-1}$, ${}^{\text{WT}}k_1^{\text{im}} = 50 \pm 5 \text{ s}^{-1}$, and ${}^{\text{WT}}K^{\text{imH}} = 0.08 \pm 0.01$. (ii) The imidazole form of wild-type cofactor is

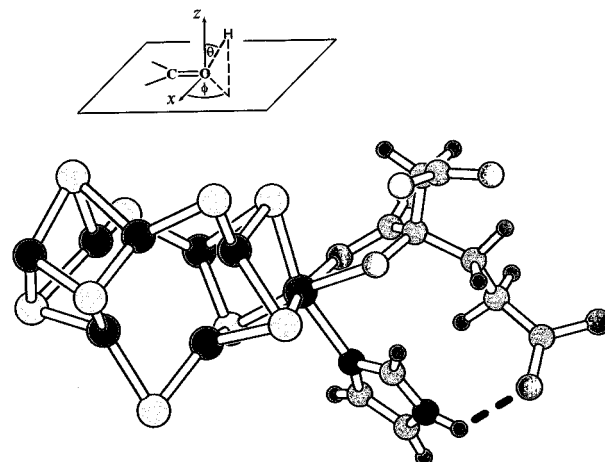


Figure 7. Optimized structure from molecular mechanics modeling studies for hydrogen bonding between imidazole and R-homocitrate in wild-type cofactor. Hydrogen bond is shown as a dotted line. For the distances and angles in this structure, see Table 1. Also shown is a diagram defining θ_{H} and ϕ_{H} .

substitutionally more labile than the analogous NifV⁻ cofactor. Clearly, when imidazole is bound to the cofactors (and only in the presence of this ligand), the reactivity of the cluster responds to citrate and homocitrate differently. Consideration of the structures of the two cofactors reveals how this may be accomplished.

Molecular mechanic calculations show that the pendant CH₂–CH₂CO₂ arm of R-homocitrate is sufficiently long and flexible that it can form a hydrogen bond with the NH group of the imidazole ligand (Figure 7). In modeling the geometry of this and other hydrogen-bonding interactions (see below), we used the work of Taylor et al.²⁵ as a guide. The imidazole ligand in the model structure of Figure 7 was generated by editing His α 442 from the crystal structure of the MoFe-protein¹⁵ and adding hydrogen atoms. The plane of the imidazole ring relative to the Mo–N bond was adjusted such that the angle between the ring centroid and the N–Mo vector was 168° (compared to 164° in the crystal structure). The parameters characterizing this and other hydrogen bonds are given in Table 1, along with the expected literature ranges. Four of these parameters were selected for optimization of the hydrogen bond, namely the H \cdots O distance, the NH \cdots O and CO \cdots H angles, and the H \cdots OCO torsion angle. For the sake of comparison, the N \cdots O distance and the angles θ_{H} and ϕ_{H} (as defined by Taylor et al.²⁵ and illustrated in Figure 7) are also included in Table 1. The parameters for the imidazole–homocitrate interaction in the model of the extracted cofactor correlate well with the given ranges for intramolecular hydrogen bonds. It should be noted that this interaction is possible because of the free rotation of imidazole about the axis of the Mo–N bond. Thus, the C ϵ 1–N δ 1–Mo–O(alkoxide) torsion angle in the model structure in Figure 7 is 39°, compared to 69° in the crystal structure of the enzyme.

In this orientation, the carboxylate group effectively acts as a base and imposes imidazolite character on the imidazole ligand. This perturbs the electron distribution within the cluster core and, hence, affects the lability of the Fe–NMF bond. In contrast, the analogous CH₂CO₂ pendant arm of citrate in the mutant cofactor is shorter and cannot interact with the imidazole ligand.

(25) Taylor, R.; Kennard, O.; Versichel, W. *J. Am. Chem. Soc.* **1983**, *105*, 5761. Taylor, R.; Kennard, O.; Versichel, W. *Acta Crystallogr.* **1984**, *B40*, 280.

Table 1. Hydrogen Bonds Involved in the Computational Models^a

bond	distances/Å		angles/deg		torsion/deg	$\theta_{\text{H}}/\text{deg}$	$\phi_{\text{H}}/\text{deg}$
	H···O	N···O	NH···O	CO···H	H···OCO		
intermolecular range ^b	1.64–2.19	2.67–3.12	150–180			56–90	20–70
intramolecular range ^b	1.66–2.32	2.47–3.04	100–150			59–90	–20–30
model imidazole–hca ^c	1.98	2.50	111	138	179	89	48
“X-ray” Ile α 425–hca	1.89	2.84	166	130	–1	90	40
“X-ray” Gln α 191–hca	1.94	2.83	152	140	–6	86	50
model Gln α 191–hca	1.90	2.81	154	143	–176	87	53
model Lys α 426–hca	1.97	2.72	131	128	158	73	40
model His α 442–hca	1.99	2.59	118	131	–176	87	42

^a Values for θ_{H} and ϕ_{H} for the individual hydrogen bonds were derived from the CO···H angle and H···OCO torsion by trigonometry. ^b Values in these rows were derived from ref 25; distance ranges were calculated as mean value $\pm 2\sigma$, angle ranges taken such that ca. 80% of values fall within the range. ^c hca = homocitrate. ^d After addition of H and manual optimization of the hydrogen-bonding contact.

It is important to note that the solvent in these studies is NMF (containing some water) and that these components could hydrogen bond to the imidazole ligand. It is conceivable that such molecules could form an extended array which “bridges” between the carboxylate group of citrate and the imidazole N–H residue. In such an extended structure, it is expected that the base strength of the carboxylate group would be appreciably diminished. The important geometrical feature of our model is that only with R-homocitrate is the carboxylate correctly positioned to interact *directly* with the imidazole N–H group.

This hydrogen bonding is consistent with two other observations concerning the reactivities of the two cofactors: (i) the substitution lability of wild-type imidazole cofactor is similar to that of NifV[–] imidazole cofactor and (ii) deprotonation of imidazole bound to wild-type cofactor ($^{\text{WT}}K^{\text{imH}} = 0.08$) is more difficult than the deprotonation of imidazole bound to NifV[–] cofactor ($^{\text{V}}K^{\text{imH}} = 0.35$). Similar effects on acidity in hydrogen-bonded molecules have been noted.²⁶

Interestingly, at high [PhS[–]]/[PhSH], the reactivities of the wild-type and NifV[–] imidazole cofactors are not the same, and the wild-type reactivity approaches that of the cofactor without imidazole bound. This behavior is not seen for the NifV[–] cofactor and is clearly dependent on the R-homocitrate. It seems likely that the negative charges on the homocitrate and imidazole ligands lead to repulsion and possibly dissociation of the imidazole ligand in the wild-type cofactor.

Parenthetically, it is worth comparing the effect of protonating the imidazole ligand with binding a proton elsewhere on the cluster. As shown in Figure 4, the protonation of the cofactors by [NHEt₃]⁺ results in an increased rate of reaction with PhSH. This behavior is similar to that observed with all synthetic Fe–S-based clusters that we have studied to date. In the synthetic clusters, the site of protonation is probably a bridging sulfur atom.²⁷ It seems likely that [NHEt₃]⁺ is also protonating a sulfur of FeMo-cofactor. However, with cofactor, it is possible that an oxygen of the polycarboxylate ligand is the site of protonation. Whichever is the case, it is clear that protonation of the coordinated imidazole has a markedly different effect than protonation of other sites on the cluster.

It is particularly noteworthy that the only conditions under which there is a difference in the reactivities of wild-type and NifV[–]-extracted cofactors is when we bind to Mo the ligand

that nature uses: in the MoFe-protein, the imidazole residue of His α 442 is coordinated at this site. How does this relate to the phenotypes of the wild-type and NifV[–] nitrogenases? It is our hypothesis that hydrogen bonding between the R-homocitrate and imidazole ligands is crucial for nitrogen fixation. In the next section, we explore this concept using the published crystallographic data for the MoFe-protein and molecular mechanics calculations.

Relevance to Enzymology. The X-ray crystal structure^{2,15} of the MoFe-protein shows that there is no hydrogen bond between the CH₂CH₂CO₂ arm of the R-homocitrate and the imidazole residue of His α 442. Rather, the carboxylate group and imidazole are “stacked”, with the carboxylate group of the CH₂CH₂CO₂ arm hydrogen bonded to the backbone NH atom of Ile α 425 (N···O distance = 2.98 Å; X-ray structure). Details of relevant hydrogen bonds from the crystal structure are also included in Table 1 to allow a fair comparison with the model structure we will describe below. The values given were obtained after adjustment of the homocitrate torsion angles to optimize the hydrogen-bonding geometry.

Although there is no hydrogen bonding between His α 442 and homocitrate in the crystal structure, this does not obviate our hypothesis since what we are proposing is a dynamic hydrogen bond which can be “switched on and off”, in tune with the electronic status/requirements of the cofactor during turnover. The crystal structure then corresponds to the “switched off” state of this interaction.

Under what conditions could the homocitrate–His α 442 hydrogen bond be “switched on”? As noted above, in the studies with extracted FeMo-cofactor in the presence of imidazole, formation of the hydrogen bond requires a significant rotation of the imidazole ring about the Mo–N bond. In the protein, the orientation of the imidazole moiety of His α 442 is defined by the conformations of the polypeptide. To undergo a rotation similar to that calculated for the untethered imidazole ligand on extracted FeMo-cofactor, significant changes involving the protein backbone would be required. His α 442 lies in a loop of three residues joining short sections of α -helix (residues 444–446) and β -sheet (residues 437–440). Although it is conceivable that this part of the protein could undergo reorganization to allow hydrogen bond formation, we have been unable to model such a change, and our attempts to do so suggest that the movements involved would be quite drastic. Given that His α 442 is unlikely to be capable of such substantial movement, the only other obvious way that the homocitrate–His α 442 hydrogen bond can be formed is by significant movement of the homocitrate.

(26) This effect of intramolecular hydrogen bonding on the acidity of the coordinated imidazole N–H is similar to that observed for the second pK_a's of maleic and fumaric acids, where the cyclic system of maleic monoanion makes it more difficult to deprotonate than the noncyclic, non-hydrogen-bonded fumarate analogue (e.g., see: Sykes, P. *A Guidebook to Mechanisms in Organic Chemistry*, 3rd ed.; Longmans: London, 1970; p 62).

(27) Henderson, R. A.; Oglieve, K. E. *J. Chem. Soc., Dalton Trans.* **1998**, 1731.

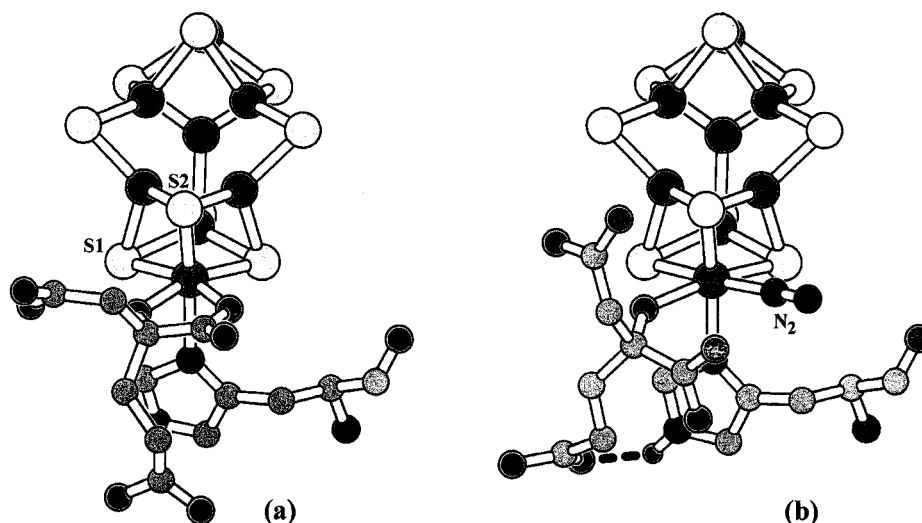


Figure 8. (a) Structure of the FeMo-cofactor in the protein, showing the orientation of the R-homocitrate and His α 442 ligands on Mo established by crystallography. (b) Proposed N₂ binding state of FeMo-cofactor, showing (i) monodentate R-homocitrate ligand, (ii) N₂ bound at vacant site on Mo, and (iii) hydrogen bond between R-homocitrate and imidazole residue. This structure is that optimized using molecular mechanics calculations. See Table 1 for hydrogen-bonding dimensions and angles.

From studies on model complexes, it has been proposed²⁸ that the homocitrate ligand could become monodentate during nitrogenase turnover, via cleavage of the molybdenum–carboxylate bond. This would open up a vacant site at molybdenum, suitable for binding dinitrogen. Applying this idea to the problem at hand, we find that *monodentate* homocitrate is able to establish a hydrogen bond between the carboxylate group of the CH₂CH₂CO₂ and the NH group of His α 442, without the imidazole moiety changing its orientation. We have developed a model of substrate-bound nitrogenase on this basis, which we now describe.

Focusing initially on the homocitrate itself, Figure 8a shows the disposition of the homocitrate–His α 442 as observed in the X-ray crystal structure, and Figure 8b shows that in our chelate ring-opened model. In the protein model, the angle between the imidazole ring centroid and the N–Mo vector was changed to 171° (from 164°) by temporarily removing the Mo–N(His α 442) bond and rotating about the histidine CH₂ group. This gave a slightly longer Mo–N bond length of 2.21 Å (compared to 2.13 Å in the crystal structure). Apart from these changes and the alterations to the Mo–O–C(homocitrate) geometry described below, the only other structural parameters varied in the modeling studies were torsion angles.

The monodentate homocitrate can best be considered as a relatively bulky alkoxide, where the geometric restraints of the chelate ring have been lost. Inspection of a number of X-ray crystal structures of molybdenum alkoxide complexes²⁹ shows that the Mo–O bond distance is typically 1.9–2.1 Å, with Mo–O–C angles in the range of 120–135°, rising to as much as ca. 150° for *tert*-butoxide complexes. We used values of 2.05 Å and 136°, respectively, for these parameters in our model

(the X-ray crystal structure values in the chelate ring are 2.00 Å and 128°, respectively). The other angles associated with the remaining Mo–O bond were also adjusted, such that N(His)–Mo–O, S1–Mo–O, and S2–Mo–O were 82, 75, and 87°, respectively, compared to 78, 89, and 84°, respectively, in the crystal structure (see Figure 8a for the sulfur labeling scheme). Having broken the molybdenum–carboxylate bond, the homocitrate is free to rotate, either clockwise or counterclockwise with respect to the molybdenum–alkoxide bond when viewed from O toward Mo. Counterclockwise rotation seems unlikely, since this would move the CH₂CH₂CO₂ arm of homocitrate away from the NH group of His α 442 and also disrupt the Gln α 191–homocitrate hydrogen bond observed in the crystal structure (Table 1 and Figure 9). Clockwise rotation, on the other hand, allows this hydrogen bond to be maintained via concerted rotation of the homocitrate CH₂CO₂ arm. The other protein–homocitrate hydrogen bond observed in the crystal structure, between the CH₂CH₂CO₂ arm and Ile α 425, is disrupted by clockwise homocitrate rotation. However, as this bond is broken, the side chain nitrogen of the next protein residue, Lys α 426, is ideally placed to form a new hydrogen bond to the other oxygen of the CH₂CH₂CO₂ carboxylate. In the crystal structure, this nitrogen atom is located 4.10 Å from the carboxylate oxygen of the homocitrate CH₂CH₂CO₂ arm, and rotation of homocitrate rapidly reduces this to hydrogen-bonding ranges. We note that this lysine is conserved in all known nitrogenases. The new hydrogen bond to Lys α 426 then acts as an anchor point to bring the homocitrate CH₂CH₂CO₂ arm into the correct position to hydrogen bond to His α 442 (Figures 8b and 9b).

A number of other salient features emerge from the model. First, the vacant site on molybdenum, resulting from the switch to monodentate homocitrate, is suitable for binding dinitrogen, as shown in Figures 8(b) and 9(b). Second, as mentioned above, the hydrogen bond from the homocitrate CH₂CO₂ arm to the side chain nitrogen of Gln α 191 is retained in the model, principally by rotation of the CH₂CO₂ arm (Table 1), with only a small change in the Gln α 191 side chain. We note that Gln α 191 is essential for nitrogen fixation. The mutant nitrogenase in which this residue has been replaced by Lys does not fix dinitrogen.³⁰ The crystal structure shows that Gln α 191

(28) Pickett, C. J. *J. Bioinorg. Chem.* **1996**, *1*, 601 and references therein.

(29) McKee, V.; Wilkins, C. J. *J. Chem. Soc., Dalton Trans.* **1987**, 523. Chisholm, M. H.; Foltling, K.; Huffman, J. C.; Putlina, E. F.; Streib, W. E.; Tatz, R. *J. Inorg. Chem.* **1993**, *32*, 3771. Bürger, K. S.; Haselhorst, G.; Stötzl, S.; Weyhermüller, T.; Wieghardt, K.; Nuber, B. *J. Chem. Soc., Dalton Trans.* **1993**, 1987. Chisholm, M. H.; Huffman, J. C.; Marchant, N. S. *Organometallics* **1987**, *6*, 1073. Bazan, G. C.; Khosravi, E.; Schrock, R. R.; Feast, W. J.; Gibson, V. C.; O'Regan, M. B.; Thomas, J. K.; Davis, W. M. *J. Am. Chem. Soc.* **1990**, *112*, 8378. Bazan, G. C.; Oskam, J. H.; Cho, H.-N.; Park, L. Y.; Schrock, R. R. *J. Am. Chem. Soc.* **1991**, *113*, 6899. Bazan, G. C.; Schrock, R. R.; O'Regan, M. B. *Organometallics* **1991**, *10*, 1062. Schrock, R. R.; Crowe, W. E.; Bazan, G. C.; DiMare, M.; O'Regan, M. B.; Schofield, M. H. *Organometallics* **1991**, *10*, 1832.

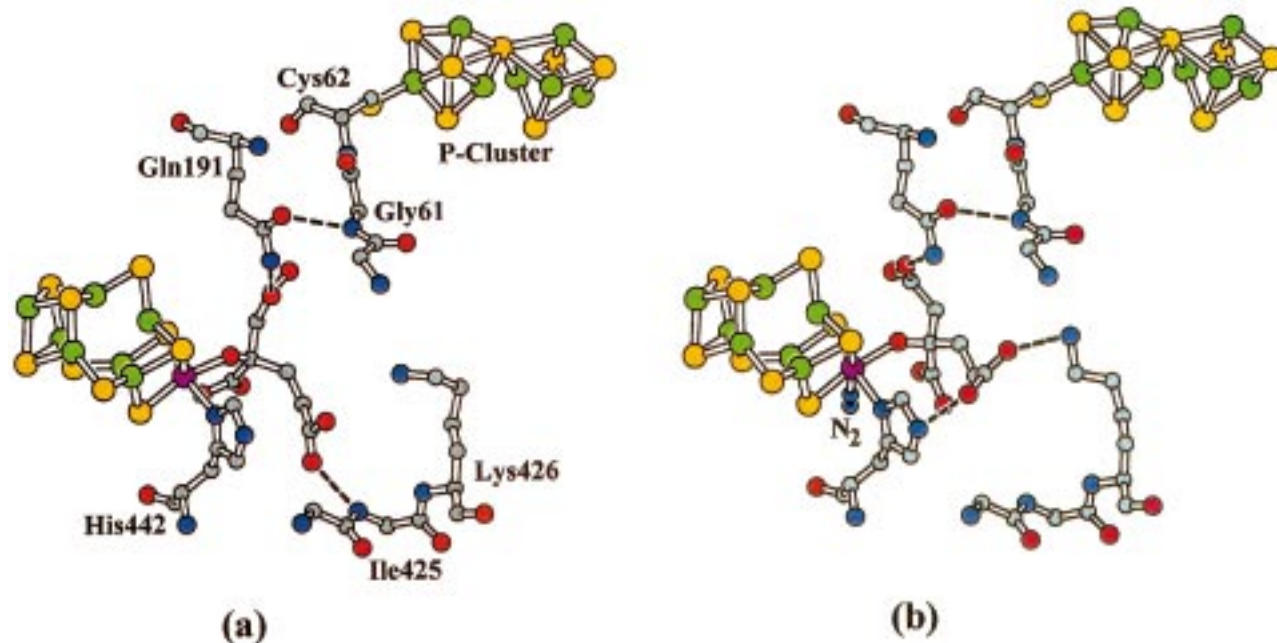


Figure 9. (a) Hydrogen-bonding network in the vicinity of the R-homocitrate ligand as established by crystallography. (b) Proposed hydrogen-bonding network in the same region after the carboxylate group of R-homocitrate has dissociated from Mo and N₂ has bound. This structure is that optimized by molecular mechanics calculations. See Table 1 for hydrogen-bonding dimensions and angles.

hydrogen bonds to homocitrate through its side-chain nitrogen, and, in addition, the side chain oxygen of Gln α 191 is hydrogen bonded to the backbone nitrogen of Gly α 61 (O–N distance = 2.80 Å).² In our model, the O ϵ 1 oxygen of Gln α 191 is displaced by just 0.15 Å from its original position; hence, this hydrogen bond is also retained. The adjacent residue, Cys α 62, is directly bonded to the P-cluster through sulfur (Figure 9). This suggests that the switching of homocitrate to a monodentate coordination mode could trigger (or be triggered by) changes at the P-cluster via the homocitrate–Gln α 191–Gly α 61–Cys α 62 hydrogen bond network. Finally, if the CO₂ arm of homocitrate has dissociated from molybdenum with concomitant protonation, the resulting CO₂H group would be well placed to donate a proton to the incoming dinitrogen ligand.

A notable feature of the nitrogenase crystal structure is the concentration of water molecules in the vicinity the homocitrate.² This allows movement of homocitrate with minimal perturbation of the protein. None of the atoms in the polypeptide backbone have been moved in our model structure. The closest non-bonding contact which has been introduced is between a homocitrate oxygen and the oxygen of Ile α 59 (2.71 Å). Moreover, the only other side chain, in addition to those of Gln α 191, Lys α 426, and His α 442, which has been changed in the model is that of Glu α 380. Rotation of this side chain is required to relieve close contacts between its carboxylate group and that of the homocitrate CH₂CH₂CO₂ arm in its new position. Given the margin of error inherent in the crystal structure and also the flexibility of the protein in vivo, any attempt to calculate the overall energy changes involved in switching from the X-ray to the model structure, we believe, would be meaningless. Nevertheless, leaving aside the role played by water molecules, the model calls for the exchange of one chemical bond for another [Mo–O (homocitrate) for Mo–N (dinitrogen)] and one hydrogen bond for two others (homocitrate–Ile α 425 for homocitrate–Lys α 426 and homocitrate–His α 442), plus changes in torsion angles and nonbonded contacts. The total energy change in switching between the two states may, therefore, be quite small.

Our calculations indicate a mechanism in which appreciable movements of the R-homocitrate ligand are “guided” by a network of hydrogen bonds from amino acid residues, which essentially do not change their positions. This is consistent with two other recent observations. First, the X-ray crystal structure of the putative transition-state complex,³¹ formed between the MoFe-protein, the Fe-protein, and MgADP·AlF₄, shows that the MoFe-protein polypeptide conformations are unperturbed from those of the isolated protein. Second, ENDOR experiments³² have shown that nonexchangeable hydrogens in the vicinity of FeMo-cofactor are rearranged in the putative transition-state complex, compared to the uncomplexed MoFe-protein.

The in vitro syntheses of nitrogenases containing various homocitrate derivatives and analogues have been reported, and the effect on the enzymes’ substrate specificity has been described.³³ Understanding most of these rather subtle effects using our molecular modeling approach is currently beyond our modeling capabilities. However, there are some rather general features which are worthy of note. A key feature of our mechanism is the hydrogen-bonding network which holds, orientates, and mediates the movement of the homocitrate. If this network is disrupted in any way, then we would expect it to modulate the movement of the homocitrate and, hence, perturb the enzyme’s activity. It seems likely that electronegative O or F substituents on homocitrate derivatives or analogues could hydrogen bond to just those amino acid residues which hydrogen bond the carboxylate groups of homocitrate and affect the activity of the enzyme.

A particularly interesting observation³⁴ is that *threo*-fluoro-homocitrate {HOC(CO₂H)(CH₂CH₂CO₂H)(CHF₂CO₂H)} forms

(30) Newton, W. E.; Dean, D. R. *ACS Symp. Ser.* **1993**, 535, 216.

(31) Schindelin, H.; Kisker, C.; Schlessman, J. L.; Howard, J. B.; Rees, D. C. *Nature* **1997**, 387, 370.

(32) Lowe, D. J.; Mitchell, C. J. Abstracts from Conference on *Nitrogen Assimilation: Molecular and Genetic Aspects*, University of South Florida, May 1997.

(33) Allen, R. M.; Chatterjee, R.; Madden, M. S.; Ludden, P. W.; Shah, V. K. *Crit. Rev. Biotechnol.* **1994**, 14, 225 and references therein.

(34) Madden, M. S.; Paustian, T. D.; Ludden, P. W.; Shah, V. K. *J. Bacteriol.* **1991**, 173, 5403.

a nitrogenase which does not sustain nitrogen fixation, but the *erythro*-fluorohomocitrate has a nitrogen fixing activity which is 25–30% of the wild-type. It is difficult to envisage that this difference arises from different electronic properties of the two diastereoisomers. However, our model suggests a more reasonable explanation. Inside the enzyme, the different dispositions of the F group in the two diastereoisomers could differentiate their reactivities, by the F in one of the isomers preferentially hydrogen bonding to the protein. It is worth emphasizing that our model involves movement of the CH₂CO₂ arm of homocitrate relative to Gln191. It is perhaps not surprising, therefore, that changes in the structure of the homocitrate in this region would affect the reactivity.

In this paper, we have seen that forming a hydrogen bond between R-homocitrate and the imidazole residue of His α 442 could effectively release electron density into the cluster. But what use would this be to nitrogenase? To understand this, it is useful to consider all the hydrogen bonding to FeMo-cofactor in the protein.

Apart from the interaction highlighted in this report, there are a number of hydrogen bonds between the cofactor and the positively charged amino acid side chains Arg α 96, Arg α 359, and His α 195 which have been identified from the crystallography. If these hydrogen bonds are dynamic, they can be used as “switches” which modulate the electron distribution within the cluster and, hence, its reactivity. By “switching on” or “switching off” the hydrogen bonds, the reactivity of the cluster can be tuned in response to the requirements of the cluster during turnover. As an example of how such a switch could be employed, we will briefly consider what must be the initial stages in nitrogen fixation: the binding and initial protonation of bound dinitrogen.

Studies on structurally defined dinitrogen complexes³⁵ have

(35) Evans, D. J.; Henderson, R. A.; Smith, B. E. In *Bioinorganic Catalysis*; Reedijk, J., Ed.; Marcel Dekker: New York, 1993; p 89 and references therein.

shown that the binding of dinitrogen to a metal site, and the ability of that dinitrogen ligand to be protonated, are favored by electron-rich sites. In simple chemical systems, the electron-richness of the site is often varied by changing the ligands on the metal. However, for FeMo-cofactor, the electron-richness of the cluster could be increased by removing electron-withdrawing hydrogen-bonding interactions from positively charged amino acid side chains and/or introducing electron-releasing hydrogen-bonding interactions from negatively charged residues (such as that described herein). In this way, the FeMo-cofactor in the enzyme can modulate its reactivity to accommodate the binding and protonation of dinitrogen.

Conclusion

In this paper, we have presented evidence that, in extracted wild-type FeMo-cofactor, hydrogen bonding between the R-homocitrate and imidazole ligands on molybdenum can perturb the reactivity of the cluster core. Using molecular mechanics calculations, we have explored this concept and its potential role in nitrogen fixation by the functioning enzyme. This is not the only proposal that has been put forward as the role for R-homocitrate. Apart from the suggestion that molybdenum–carboxylate dissociation is a prerequisite to dinitrogen binding²⁸ (which we have already discussed and accommodated in our model), it has also been proposed that homocitrate is a component of the proton delivery system.³⁶ However, only our proposal rationalizes why R-homocitrate, and not closely related organic acids, is peculiarly advantageous for nitrogen fixation.

Acknowledgment. We thank the BBSRC for supporting this work and John Innes Foundation for a studentship (K.L.C.G.). We thank Drs. Bob Eady, David Hughes, David Lawson, David Lowe, and Chris Pickett for helpful discussions.

JA981832O

(36) Coucouvanis, D. *J. Bioinorg. Chem.* **1996**, *1*, 594 and references therein.